Babol University of Medical Sciences
IJMCM
International Journal of Molecular and Cellular Medicine
p-ISSN: 2251-9637 o-ISSN: 2251-9645
Cellular and Molecular Biology Research Center

Optimization of Fluorapatite/Bioactive Glass Nanocomposite Foams as Bone Tissue Scaffold: An in Vivo Study

Seyedali Seyedmajidi[1*], Maryam Seyedmajidi[1], Sina Haghanifar[2]

1. Dental Materials Research Center, Health Research Institute, Babol University of Medical Sciences, Babol, Iran.
2. Oral Health Research Center, Health Research Institute, Babol University of Medical Sciences, Babol, Iran.

Article type: **Original Article**

Received: 2024.03.24
Revised: 2024.04.29
Accepted: 2024.05.01

ABSTRACT

The present study investigated the suitability of nanocomposite foams of fluorapatite and bioactive glass (FA /BG) in different weight ratios as scaffolds for bone tissue in rat tibia regeneration to determine the optimal composition. FA and BG nano powders with a weight ratio of 25% FA/75% BG (compound 1) and 75% FA/25% BG (compound 2) were used as precursors for gel casting to produce nanocomposite foams. Thirty rats were randomly divided into two equal groups. Disk-shaped samples of each compound were implanted into the tibias of 15 rats. After 15, 30, or 60 days, five rats from each group were sacrificed and subjected to radiological, histopathological, and histomorphometrical examination. Data were analyzed using SPSS software. No foreign body reaction was observed in either group at all intervals, and the bone-biomaterial junction was direct. Overall, the inflammation rate, and the number of blood vessels, osteoblasts, and osteoclasts decreased over time in both groups. However, the number of osteocytes, trabecular bone thickness, and the percentage of new bone formation increased, in contrast to the remaining biomaterial percentage. Most of the changes in the group implanted with compound 2 were significantly more significant and faster than in the other group. Although the composite with the higher percentage of FA was superior to the composite with the higher percentage of BG, considering the results of our previous similar studies, the composite with the same percentage of FA and BG is more favorable to be used as a substitute for bone tissue in the body.

Keywords: Fluorapatite, 58S bioactive glass, nanocomposite, tissue engineering

Cite this article: Seyedmajidi SA, *et al*. Optimization of Fluorapatite/Bioactive Glass Nanocomposite Foams as Bone Tissue Scaffold: An in Vivo Study. *International Journal of Molecular and Cellular Medicine*. 2023; 12(4):388-400. **DOI:** 10.22088/IJMCM.BUMS.12.4.388

*Corresponding: Seyedali Seyedmajidi
Address: Dental Materials Research Center, Health Research Institute, Babol University of Medical Sciences, Babol, I.R.Iran.
E-mail: s.majidi.dvm@gmail.com

Introduction

The increasing need for bone tissue replacement and the limitations of conventional methods (autografts, allografts, and xenografts) such as low availability, lack of mechanical strength, malleability, disease transmission, and immunological responses have led specialists to use synthetic materials composed of metals, ceramics, polymers, and composites (1, 2). To achieve complete regeneration and recovery, the production of new osteoconductive and osteoinductive biomaterials to enhance and control complete tissue regeneration is of paramount importance (3).

Calcium phosphate ceramics, especially hydroxyapatite (HA), are widely used as bone replacement implants and for the fabrication of porous tissue scaffolds because of their bone-like chemical composition and excellent biological properties, including biocompatibility and osteoconductivity (4-10). The use of these bio-ceramics has been limited because of their fragility and low strength (11). To overcome this shortcoming, fluorapatite-containing composites have been developed for medical applications (12). When the OH^- groups are completely replaced by F^-, fluorapatite (FA) $Ca_{10}(PO_4)_6F_2$ is formed (13). FA is known for its advantages such as chemical stability and its ability to retard the decay process (14). It is also less soluble than HA (15). Another advantage of fluoride-doped apatite is the development of biomaterials that can release fluoride ions (16). According to the guidelines of WHO, F^- is required to prevent dental caries and promote healthy bone growth (17). Several studies have shown that the amount of fluoride ions released directly affects cell attachment, proliferation, morphology, and differentiation of osteoblast cells and increases mineralization and crystallization (18, 19). In addition, F^- causes stronger cell attachment through better protein uptake and increases phosphate activity, thereby increasing osteoconductivity (19-22). Some articles have cited higher fluoride concentrations as a cause of side effects such as osteomalacia, decreased osteoconductivity (23), and bone mechanical properties (24).

Bioactive glasses have the ability to stimulate cells by releasing ionic products during their biodegradation process. This release of ions enhances the proliferation of human osteoblasts and triggers the expression of insulin-like growth factor II mRNA and protein synthesis. Consequently, a stable connection is formed with the surrounding tissues (25). Bioactive glass (BG), comprising of compounds such as CaO, SiO_2, and P_2O_5, has the unique capability to bind to both soft and hard tissues without any need for a connective tissue (26, 27). It is particularly remarkable for its ability to create strong interfacial bonds with the surrounding tissues (28). However, the inherent fragility of glass poses a limitation in using bioactive glass as a scaffold in tissue engineering applications (29).

By combining BG particles with FA, unique properties such as enhanced bioactivity and improved mechanical characteristics can be achieved (30, 31). If this combination is optimized in a tissue engineering scaffold, the resulting composite offers a remarkable opportunity to create scaffolds with suitable physico-mechanical and biological properties, effectively matching the rate of biodegradation with new bone formation in the human body. Currently, there are several technologies available for producing porous bio-ceramic scaffolds, one of which is the gel casting method. This particular approach is suitable for manufacturing ceramic scaffolds that exhibit high strength, dimensional accuracy, a uniform structure, and complex shapes (29, 32).

Based on the findings from our previous research, which focused on studying nanocomposite foams comprising of apatite and BG in equal weight ratios as potential cell scaffolds for bone tissue replacement, we have identified the superiority of the FA/BG composition over HA/BG and CenoBone® (1). Therefore, the objective of our current study is to utilize FA/BG nanocomposite foam with varying weight ratios, produced through gel casting, as a cell scaffold to repair tissue in rat's tibia bone defect. Through this study, we aim to identify the optimal composition that exhibits the maximum tissue repair ability.

Materials and methods

Preparation of FA/BG Nanocomposite Foam

Nanopowders of FA and BG 58S with a composition of 58%SiO_2, 36%CaO, 6%P_2O_5 (Nikceram Razi, Isfahan, Iran) with a particle size of <100 nm made by the sol-gel method were used as a precursor of nanocomposite foams. In the gel casting process, agarose powder (Merck, Darmstadt, Germany), Tergitol Np-9 (Sigma-Aldrich, St. Louis, MO, USA), and sodium tripolyphosphate (TPP; Sigma-Aldrich) were employed.

FA and BG Nano powders with a weight ratio of 25%FA/75%BG (compound 1) and 75%FA/25%BG (compound 2) were mixed. Each compound was added 60 wt% to 1 wt% TPP solution in deionized water, and the mixture was stirred for 15 minutes using a magnetic stirrer. Subsequently, a 7 wt% agarose solution was added to the mixture and stirred at 130°C as long as a composition of 50 wt% FA/BG and 1.2 wt% agarose was obtained. Finally, 3 vol% Tergitol was added as a surfactant to the suspension, and the foaming process was carried out using a three-blade stirrer at 80°C. The resulting product was poured into polyethylene containers with dimensions of 2 mm in diameter and 3 mm in height. Gelation was achieved by cooling the containers to 0°C. The samples were then removed from the mold, dried at room temperature, and finally sintered in an electric furnace at 1200°C for 4 h (33).

Since the composite with equal amounts of FA and BG was already investigated in our previous study (1), we decided to adhere to ethical standards in biological research and avoid subjecting laboratory animals to unnecessary experiments. As suggested by the ethics committee, we did not repeat the experiments on the composition with equal weight ratios and the control group. Therefore, the results obtained from our previous research were used for comparison in the discussion.

Implantation in Animals

Before implantation, the sintered nanocomposite foams underwent autoclaving and were then stored in sterile containers.

Animal Preparation

After obtaining approval from the research ethics committee (IR.MUBABOL.REC.1399.063), the experiments were conducted on the right tibia of thirty male Wistar rats aged between 10-12 weeks, weighing between 300-400 g. The rats were housed individually in standard-sized stainless-steel cages to limit movement and prevent excessive pressure on the surgical site. All surgeries were performed in a dedicated sterile room. The animals were anesthetized by intraperitoneal injection, using a combination of 2 ml of ketamine (100 mg/ml) and 1 ml of xylazine (20 mg/ml). Once the animal was under deep anesthesia,

the inner surface of its right foot was shaved and subsequently washed with 70% isopropanol and scrubbed with betadine (1).

Implantation

A full-thickness 1.5 cm longitudinal incision was made on the skin of the middle third of the inner surface of the tibia. Carefully, a fine retractor was used to open the skin incision, exposing the tibia. Next, the surface of the tibia was thoroughly cleansed of any connective tissues.

Using a trephine bur with a 2 mm diameter, which was connected to a micromotor operating at a speed of 2000 rpm, a defect was created that extended into the bone marrow. Throughout the process, normal saline was used for irrigation. Following this, the site of the defect was delicately cleaned of any blood and bone fragments, utilizing suction. Finally, nanocomposite foams were inserted into the defects with gentle pressure (1). The rats were divided randomly into two equal groups (n=15 per group). In the first group, compound 1 was utilized to fill the bone defects, while in the second group, compound 2 was used.

If necessary, the muscles were first fixed using 4-0 absorbable sutures, and then the skin incision was sutured using 4-0 non-absorbable sutures. To replenish the lost fluids during the surgery, each rat received an intraperitoneal injection of 5 ml of 5% glucose-saline solution.

After 15, 30, or 60 days, five rats from each group were sacrificed with a high-dose intraperitoneal injection of pentobarbital. The tibia bone, along with the surrounding soft tissue, was extracted and fixed in 10% formaldehyde buffer solution at pH=7.4 for four weeks at a temperature of 4°C.

Radiographical Evaluations

Radiographs were taken by a Prostyle unit (Planmeca, Finland) under a 50 kV voltage and an 8 mA currency during 0.4 s of radiation onto a digital phosphor sensor plate (PSP) of size 3 (Sordex, Finland). The distance between the tibia and the X-ray tube was 50 cm. PSPs were processed using PCT (Sordex, Finland). To analyze the density, five points were selected at both the implant site and the healthy part of the tibia. The density measurements were conducted using Digora software version 2.5. The mean density difference percentage between the implantation site and the healthy part of the bone were compared between two groups, as well as within each group at different time intervals (1).

Histopathological and Histomorphometrical Evaluations

Samples were decalcified in 10% nitric acid (34). After tissue passage and the preparation of paraffin blocks, serial sections with a 5 µm diameter were prepared from the defect site and stained with hematoxylin and eosin. All slices taken from the defect site were photographed with the Olympus DP12 digital camera attached to the Olympus BX41 light microscope at 400x magnification. Appropriate images were selected and analyzed with Analysis LS Starter software, which has the ability to measure distance and surface area. The inflammation status, foreign body reaction, blood vessel counts, bone viability, bone biomaterial contact, and mean bone cell (namely osteoblasts, osteoclasts, and osteocytes) counts were assessed. The thickness of bone trabeculae was measured in µm. New bone formation and residual biomaterials in defect sites were expressed as percentage of the whole field. All items evaluate under three microscopic fields of each section. The items were ranked as follows: (1)

Inflammation: Grade 0, lack of inflammatory cells; Grade 1, diffuse inflammatory cells (mild inflammation); Grade 2, 5-10 focal inflammatory cells; Grade 3, 11-50 focal inflammatory cells; Grade 4,>50 focal inflammatory cells.

Foreign body reaction: (+) the presence of giant cell granulomatous reaction; (-) absence of granulomatous reaction of giant cells.

Bone life: (+) the presence of osteocytes in Lacuna; (-) absence of osteocytes in Lacuna.

Bone-biomaterial connection mode: (+) direct contact; (-) the presence of any connective tissue between bone and biomaterial.

Statistical Analysis

The data was statistically analyzed using SPSS software version 26. Descriptive statistical parameters were used to compare the quantitative parameters between the groups in each time interval and within each group between the time intervals. A mean difference comparison analysis test and multiple comparisons were conducted, considering the parametric conditions. The significance level was set at P=0.05.

Results

Figure 1 depicts the microscopic images of rat tibia sections taken at the defect site in the studied groups and at various time intervals.

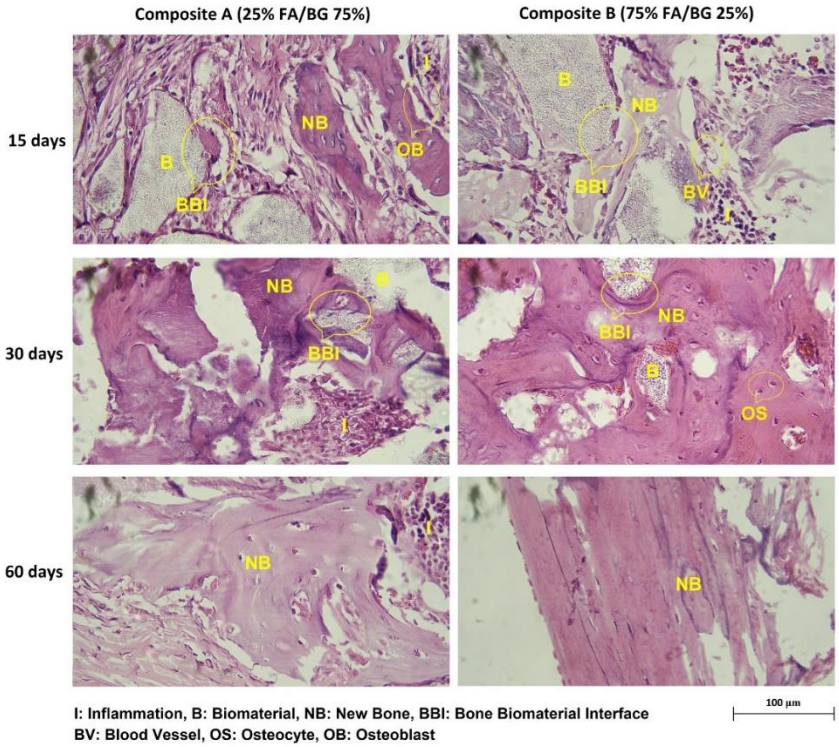

Fig. 1. Histopathologic features of the bone defect (implantation site) after 15, 30, or 60 days of scaffolds implantation in the tibia of rats (400X magnification). No foreign body response was observed; the bone-biomaterial connection was direct; blood vessels count, inflammation rate, the number of osteoblasts, osteoclasts, and osteocytes as well as trabecular bone thickness, percentage of new bone formation, and the remaining biomaterial percentage were evaluated.

Based on the analysis of the images, it was observed that there was no foreign body response in the groups as evidenced by the absence of giant cells and granulomatous reactions. The presence of osteocytes in the lacuna space in all groups indicated that the bone was alive and healthy. Moreover, the direct bone-biomaterial connection observed in both groups at all intervals, without the presence of connective tissue, further reinforces the excellent biocompatibility of the biomaterials used.

Table 1 displays the histopathological evaluation results. On day 15, group 2 exhibited a significantly higher number of blood vessels compared to group 1 (P=0.008). In terms of intragroup comparisons, both groups showed a significant decrease in the number of blood vessels over time (p<0.05), with group 2 experiencing a more pronounced decline compared to group 1 (P<0.001).

Table 1. Comparison of mean±SD of histopathological evaluation variables between groups at studied time intervals and within groups between time intervals.

Variables	Time	25%FA/BG75%	75%FA/BG25%	*P value*
Blood vessels count (n)	15	1.67 ± 0.34	3.07 ± 0.83	**0.008**
	30	1.07 ± 0.15	1.27 ± 0.6	0.498
	60	0.6 ± 0.83	0.2 ± 0.3	0.69
P value		**0.036**	**<0.001**	
Inflammation rate (grade)	15	2.47 ± 0.56	2.4 ± 0.64	0.867
	30	2.4 ± 0.15	1.26 ± 0.15	**0.008**
	60	0.73 ± 0.98	0	0.151
P value		**0.033**	**0.002**	
Osteoblasts count (n)	15	44 ± 11.53	51 ± 7.44	0.287
	30	44.89 ± 7.46	25.87 ± 8.54	**0.006**
	60	14.27 ± 5.94	7.27 ± 1.67	**0.032**
P value		**<0.001**	**<0.001**	
Osteocytes count (n)	15	24 ± 10.73	26.53 ± 9.3	0.69
	30	34.33 ± 2.63	65 ± 14.67	**0.009**
	60	49.33 ± 9.79	59.93 ± 6.02	0.073
P value		**0.002**	**<0.001**	
Osteoclasts count (n)	15	1.4 ± 0.6	0.33 ± 0.58	**0.016**
	30	0.27 ± 0.59	0.2 ± 0.3	0.841
	60	0.13 ± 0.3	0	0.69
P value		**0.008**	0.288	

The inflammation rate decreased over time in both groups and reached zero after 60 days in group 2. Comparing the two groups, it was found that after one month of implantation, the rate of inflammation was significantly lower in group 2 than in group 1 (P=0.008).

In addition, there was a notable decline in the number of osteoblasts over time. Specifically, in group 2, the decline was more rapid and significant across all three-time intervals (P<0.001). However, in group 1, the decrease was observed only between 30 and 60 days (P<0.001). When comparing the two groups after 30 and 60 days of implantation, group 2 exhibited a lower number of osteoblasts compared to group 1 P=0.006 and P=0.032, respectively).

Unlike osteoblasts, the number of osteocytes increased over time; however, the difference was not significant in group 1 between days 15 and 30 (P=0.176), but it became significant between days 30 and 60 (P=0.041). In group 2, this increase was observed in the early days of implantation, and the difference between days 15 and 30 was significant (P<0.001). However, there was no significant variation after day 30 until day 60 (P=0.736). Additionally, on day 30, the number of osteocytes was higher in group 2 compared to group 1 (P=0.009).

The number of osteoclasts decreased over time in both groups, with a significant decrease observed in group 1 between days 15 and 30 (P=0.04). In group 2, the rate of osteoclasts reached zero after 60 days. Furthermore, the number of osteoclasts was lower in group 2 compared to group 1, and this difference was significant on day 15 (P=0.016).

Table 2 presents the findings from the histomorphometrically and radiographical evaluations. The results show that trabecular bone thickness increased over time in both groups. This increase was particularly significant in group 1 between day 30 and 60 (P=0.003) and in group 2 between day 15 to 30 and day 30 to

Table 2. Comparison of mean±SD of histomorphometrical and radiographical evaluation variables between groups at studied time intervals and within groups between time intervals.

Variables	Time	25%FA/BG75%	75%FA/BG25%	*P value*
Trabecular bone thickness (µm)	15	56.1 ± 11.88	64.35 ± 14.43	0.353
	30	77.6 ± 19.76	141.93 ± 21.01	**0.001**
	60	137.44 ± 31.34	194.03 ± 42.52	**0.046**
P value		**<0.001**	**<0.001**	
New bone formation (percent)	15	14.75 ±10.56	20.07 ± 9.4	0.425
	30	32.19 ± 7.23	55.98 ± 14.14	**0.016**
	60	42.77 ± 7.21	65.85 ± 22.86	**0.032**
P value		**0.001**	**0.002**	
Remain biomaterial (percent)	15	17.53 ± 9	14.74 ± 7.69	0.612
	30	10.85 ± 2.96	10.37 ± 4.47	0.847
	60	8.24 ± 6.93	0.28 ± 0.43	**0.016**
P value		**0.124**	**0.007**	
Density increment (percent)	15	0.02 ± 0.06	0.01 ± 0.05	0.843
	30	0.03 ± 0.05	0.02 ± 0.06	0.706
	60	0.05 ± 0.05	0.04 ± 0.02	0.704
P value		0.651	0.65	

60 (*P*=0.003 and *P*=0.034, respectively). Additionally, the trabecular bone thickness was significantly higher in group 2 compared to group 1 on days 30 and 60 (*P*=0.001 and *P*=0.046, respectively).

The group 2 showed a significantly higher percentage of new bone formation compared to group 1 on days 30 and 60 (*P*=0.016 and *P*=0.032, respectively). Additionally, the amount of new bone formation increased over time, and this increase was significant between 15 and 30 days in both groups (*P*=0.018 and *P*=0.012, respectively).

The percentage of remaining biomaterial decreased significantly over time, particularly in group 2 between days 30 and 60 (*P*=0.015). Additionally, when compared to group 1, group 2 exhibited significantly lower levels of remaining biomaterial after 60 days of implantation (*P*=0.016).

Figure 2 displays the radiographic images of rat tibia in two groups taken at three different time

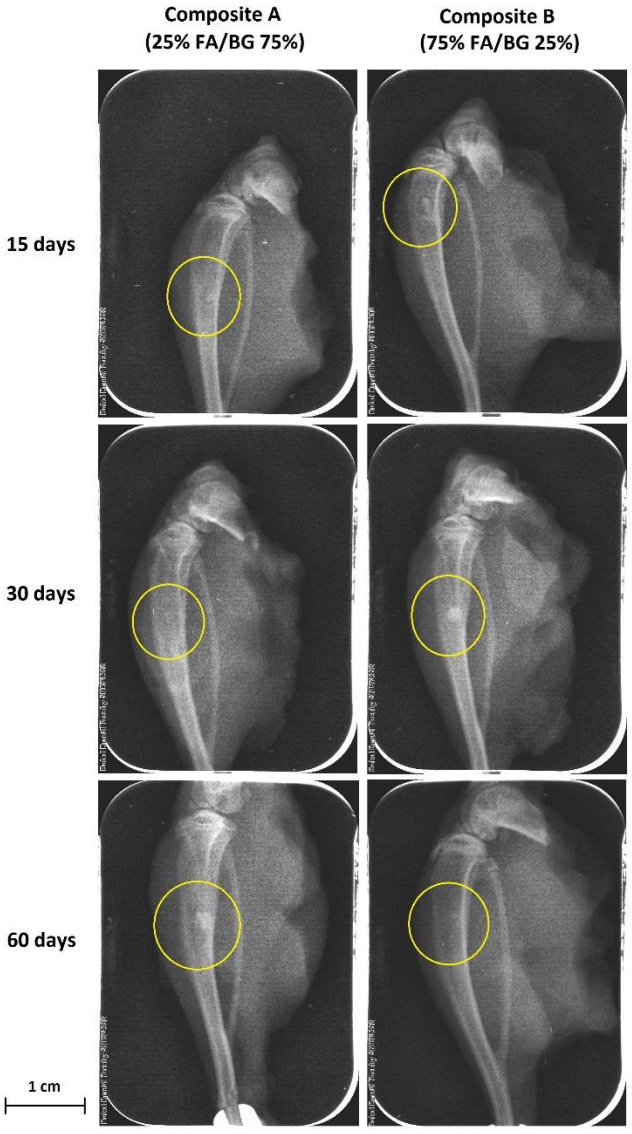

Fig. 2. Radiographic images of the tibia from each studied group at three times intervals.

intervals. The marked areas indicate the implantation sites. Our analysis found no considerable difference in the increase of bone density between the two groups. Additionally, there was no significant variation observed in the radiographic examination of the implant site throughout all time intervals.

Discussion

The gel-casting method enables the creation of macroporous scaffolds that can be tailored to fit the specific shapes and dimensions required by patients (32). By using FA and BG nanoparticles, which have a large specific surface area, the fabrication of cell scaffolds promotes and accelerates the rate of tissue regeneration. The novelty of this study was to investigate various weight ratios of FA and BG. The purpose of this study was to identify the optimal composition of FA and BG using two different weight ratios. Most of the parameters analyzed in this study indicated that the process of rat tibia bone tissue regeneration was quicker and more intense when using a compound with a higher ratio of FA.

Bio-ceramics have been found to have a positive impact on the regeneration of bone tissue, acting as a replacement material. A systematic review conducted by Brunello *et al*. investigated the effect of bio-ceramics on bone regeneration in pre-clinical *in vivo* studies between 2013 and 2018. The results demonstrated that the inclusion of bio-ceramics enhanced and expedited the process of ossification across all studies. For bone tissue substitution materials to be effective, they should possess biocompatibility, osteoconductivity, and absorbability, while also providing the necessary mechanical strength, particularly in weight-bearing areas. Ultimately, these materials should be gradually replaced by newly formed bones (35).

Numerous factors, including synthesis and construction methods, scaffold microstructure, porosity characteristics, and the preload of the scaffold with growth factors, can affect the mechanical and biological properties of scaffolds. Additionally, the type of animal model used in the study, the size of the defect, and the time of implantation can influence the *in vivo* behavior and outcomes of the scaffold (36). One of the main factors in constructing scaffolds is the presence of macro-scale porosity. Previous studies have demonstrated that having porosity within the range of 100 to 400 microns allows for the penetration of intercellular fluids, cell infiltration, and angiogenesis (1, 29). Macroporous bio-ceramic scaffolds are often created using the replica foam method. This method involves inducing and heating a polymeric foam to dry it, burn out the polymer, and sinter the particles (37).

The decrease in the number of blood vessels is time-dependent due to tissue maturation at the implant site. This finding was in agreement with the results of other studies (1, 32, 38). It seems that a higher concentration of FA promotes angiogenesis within the first two weeks post-implantation.

The gradual decrease in the inflammation rate over time suggests that the utilized composites are biocompatible. The absence of inflammation in group 2 after 60 days of implantation indicates that the compound with a higher fluorapatite content exhibits superior biocompatibility. This finding aligns with the research conducted by Mansoorifar *et al*. (39).

In agreement with the results of similar studies (1, 40), the count of osteoblasts and osteoclasts decreased over time. This decrease was faster in the group with higher levels of FA (group 2). Furthermore, the difference was more pronounced between days 15 to 30 compared to days 30 to 60. As described by

previous studies conducted by Saginoca *et al*. (40) and Seyedmajidi *et al*. (32), the bone cell variations indicate bone maturation and proliferative activity, concluded that compound 2 facilitated faster bone regeneration.

The trabecular bone thickness and rate of new bone formation increased over time in both groups. Group 2 had higher values on days 30 and 60, suggesting that the more FA led to greater ossification. In contrast, only group 2 showed a significant increase in trabecular bone thickness from day 15 to 30, indicating a more pronounced acceleration of ossification with compound 2. Macedo *et al*., in an *in vivo* study using bioactive glass for 30 days, also found thicker and more mature bone trabeculae, supporting the concept of bone remodeling (41). Additionally, Gamal Abdel Salam *et al*. observed complete formation of bony trabeculae surrounding the implant site after 30 days of applying bio-glass in rat tibia (42).

The decrease in the percentage of remaining biomaterial observed in both groups over time indicates the biodegradability of the biomaterials used. However, this decrease was found to be significant only in group 2. The lower remaining biomaterial can be attributed to the higher new bone formation and shows the greater and more intense biological activity of biomaterial (38, 43). These changes indicated that the rate of new bone formation in group 2 was significantly higher than in group 1.

The density increment of tibia at the implant site was similar in two groups at all-time intervals. However, given that the amount of the remained biomaterial at the implant site significantly decreased in group 2, the density observed at the implant site in group 2 indicates the higher ossification activity of compound 2.

Proper composition, fluoride content, and understanding of how to enter into ceramics, as well as sintering conditions, can contribute to the synthesis of ceramics with the desired attributes, such as porosity, ion adsorption capacity, bioactivity, and compatibility (16, 31). In a study conducted by Taktak *et al*., they examined the synthesis of a bio-composite comprising beta-tricalcium phosphate with 26.52% fluorapatite. The researchers investigated its potential as an alternative material for regenerating bone tissue in rabbit tibia. After six weeks of implantation, all histopathological observations indicated excellent biocompatibility and adsorption capacity of the bio-ceramic (44). Mansoorifar *et al*. conducted a study to optimize the levels of fluorine substitution in the structure of fluorhydroxyapatite. Their findings revealed that the presence of fluorine in the apatite structure enhances the production of natural apatite and improves the performance of MG-63 osteoblast-like cells. Additionally, the study observed that cell adhesion and cell density increased with higher levels of fluorine content. The ALP activity test demonstrated that mineralization ability significantly improved with increasing levels of fluorine. Furthermore, the corrosion resistance of the material was enhanced. The compound containing 75% fluorine in the apatite structure was identified as the optimal compound in terms of biocompatibility, while the compound with 100% fluorine exhibited superior corrosion resistance (39).

In our previous study comparing the effectiveness of HA/BG, FA/BG, and Cenobone® (1) composites, we concluded that the FA/BG composite (containing equal amounts of FA and BG) showed superior results. This current study focused on compounds with varying proportions of FA and BG, and it confirmed that compound 2 is definitively superior to compound 1. By comparing the results of this study with those of the previous study, we found that most of the studied parameters, such as angiogenesis, inflammation rate, and

the number of osteoblasts, yielded similar results. However, the compound with equal proportions of FA and BG demonstrated improved ossification and greater bone maturation, while also completely degrading the biomaterials. It is important to note that the scaffolding and implantation methods used in both studies were identical (1).

In the comparison of fabricated nanocomposite foams with two different weight ratios of FA and BG, although the composite containing more FA demonstrated its superiority over the composition containing more BG, the composite with equal amounts of FA and BG is more favored to be used as a substitute for bone tissue in the body, considering the results of previous similar studies.

Acknowledgments

The authors thank staff of the Dental Materials Research for their assistance during this research. This manuscript was edited for proper English language, grammar, punctuation, spelling, and overall style by qualified native English-speaking editors at NedMedica® (Heerlen, Netherlands).

Conflicts of Interest

The authors declared no potential conflicts of interest with respect to the research, authorship, and/or publication of this article.

References

1. Seyedmajidi M, Haghanifar S, Hajian-Tilaki K, et al. Histopathological, histomorphometrical, and radiological evaluations of hydroxyapatite/bioactive glass and fluorapatite/bioactive glass nanocomposite foams as cell scaffolds in rat tibia: an in vivo study. Biomed Mater 2018;13:025015.

2. Ghomi H, Fathi MH, Edris H. Fabrication and characterization of bioactive glass/hydroxyapatite nanocomposite foam by gelcasting method. Ceram Int 2011;37:1819-24.

3. Polini A, Bai H, Tomsia AP. Dental applications of nanostructured bioactive glass and its composites. Wiley Interdiscip Rev Nanomed Nanobiotechnol 2013;5:399-410.

4. Netz DJ, Sepulveda P, Pandolfelli VC, et al. Potential use of gelcasting hydroxyapatite porous ceramic as an implantable drug delivery system. Int J Pharm 2001;213:117-25.

5. Resmim CM, Dalpasquale M, Vielmo NIC, et al. Study of physico-chemical properties and in vitro antimicrobial activity of hydroxyapatites obtained from bone calcination. Prog Biomater 2019;8:1-9.

6. Szubert M, Adamska K, Szybowicz M, et al. The increase of apatite layer formation by the poly(3-hydroxybutyrate) surface modification of hydroxyapatite and beta-tricalcium phosphate. Mater Sci Eng C Mater Biol Appl 2014;34:236-44.

7. Azevedo AS, Sa MJ, Fook MV, et al. Use of chitosan and beta-tricalcium phosphate, alone and in combination, for bone healing in rabbits. J Mater Sci Mater Med 2014;25:481-6.

8. Zhang Y, Li S, Wu C. The in vitro and in vivo cementogenesis of CaMgSi(2)O(6) bioceramic scaffolds. J Biomed Mater Res A 2014;102:105-16.

9. Aktug SL, Durdu S, Yalcin E, et al. Bioactivity and biocompatibility of hydroxyapatite-based bioceramic coatings on zirconium by plasma electrolytic oxidation. Mater Sci Eng C Mater Biol Appl 2017;71:1020-7.

10. Zabihi E, Pourbagher R, Seyedmajidi SA. Cytotoxicity and Genotoxicity Evaluation of Fluorapatite/Bioactive Glass Nanocomposite Foams with Two Various Weight Ratios as Bone Tissue Scaffolds: an in vitro Study. Iran J Mater Sci Eng 2022;19.

11. Bouslama N, Chevalier Y, Bouaziz J, et al. Influence of the sintering temperature on Young's modulus and the shear modulus of tricalcium phosphate–fluorapatite composites evaluated by ultrasound techniques. Mater Chem Phys 2013;141:289-97.
12. Elghazel A, Taktak R, Bouaziz J. Determination of elastic modulus, tensile strength and fracture toughness of bioceramics using the flattened Brazilian disc specimen: analytical and numerical results. Ceram Int 2015;41:12340-8.
13. Shen J, Jin B, Jiang Qy, et al. Morphology-controlled synthesis of fluorapatite nano/microstructures via surfactant-assisted hydrothermal process. Mater Des 2016;97:204-12.
14. Ayed FB, Bouaziz J. Sintering of tricalcium phosphate–fluorapatite composites by addition of alumina. Ceram Int 2008;34: 1885-92.
15. Tredwin CJ, Young AM, Abou Neel EA, et al. Hydroxyapatite, fluor-hydroxyapatite and fluorapatite produced via the sol-gel method: dissolution behaviour and biological properties after crystallisation. J Mater Sci Mater Med 2014;25:47-53.
16. Borkowski L, Przekora A, Belcarz A, et al. Fluorapatite ceramics for bone tissue regeneration: Synthesis, characterization and assessment of biomedical potential. Mater Sci Eng C Mater Biol Appl 2020;116:111211.
17. Organization WH. Atrazine in drinking-water: background document for development of WHO guidelines for drinking-water quality: World Health Organization2003.
18. Nathanael AJ, Mangalaraj D, Hong SI, et al. Influence of fluorine substitution on the morphology and structure of hydroxyapatite nanocrystals prepared by hydrothermal method. Mater Chem Phys 2013;137:967-76.
19. Lei Z, Li F, Chen X, et al. The in vitro osteogenic and angiogenic effects of sodium-free fluoride-containing bioactive glasses. Mater Lett 2019;248:138-42.
20. Razavi M, Fathi MH, Meratian M. Fabrication and characterization of magnesium–fluorapatite nanocomposite for biomedical applications. Mater Charact 2010;61:1363-70.
21. Barandehfard F, Kianpour Rad M, Hosseinnia A, et al. The addition of synthesized hydroxyapatite and fluorapatite nanoparticles to a glass-ionomer cement for dental restoration and its effects on mechanical properties. Ceram Int 2016;42:17866-75.
22. Santos SC, Barreto LS, dos Santos EA. Nanocrystalline apatite formation on bioactive glass in a sol–gel synthesis. J Non-Cryst Solids 2016;439:30-7.
23. Qu H, Wei M. The effect of fluoride contents in fluoridated hydroxyapatite on osteoblast behavior. Acta Biomater 2006;2: 113-9.
24. Rezaee T, Bouxsein ML, Karim L. Increasing fluoride content deteriorates rat bone mechanical properties. Bone 2020;136:115369.
25. Mortazavi V, Nahrkhalaji MM, Fathi MH, et al. Antibacterial effects of sol-gel-derived bioactive glass nanoparticle on aerobic bacteria. J Biomed Mater Res A 2010;94:160-8.
26. Doostmohammadi A, Fathi MH, Bigham Sadegh A, et al. In Vivo Evaluation of Bioactive Nano Bioceramics for Incorporation into and Production of Bone (an Animal Study). Iranian Journal of Orthopedic Surgery(IJOS) 2020;10:67-76.
27. Baino F, Fiume E, Barberi J, et al. Processing methods for making porous bioactive glass-based scaffolds—A state-of-the-art review. Int J Appl Ceram 2019;16:1762-96.
28. Joughehdoust S, Manafi S. Synthesis and in vitro investigation of sol-gel derived bioglass-58S nanopowders. Mater Sci -Pol 2012;30:45-52.
29. Ghomi H, Fathi MH, Edris H. Effect of the composition of hydroxyapatite/bioactive glass nanocomposite foams on their bioactivity and mechanical properties. Mater Res Bull 2012;47:3523-32.

30. Manafi S, Mirjalili F, Reshadi R. Synthesis and evaluation of the bioactivity of fluorapatite-45S5 bioactive glass nanocomposite. Prog Biomater 2019;8:77-89.
31. Seyedmajidi SA, Seyedmajidi M. Fluorapatite: A Review of Synthesis, Properties and Medical Applications vs Hydroxyapatite. Iran mater sci eng 2022;19.
32. Seyedmajidi S, Pourbagher R, Seyedmajidi M. The effect of eliminating sintering during the synthesis of 3D scaffolds using the gel-casting method on their biological characteristics: in vivo and in vitro evaluations. Biomed Mater 2023;18:055015.
33. Seyedmajidi SA, Seyedmajidi Sk, Alaghehmand H, et al. Synthesis and characterization of hydroxyapatite/bioactive glass nanocomposite foam and fluorapatite/bioactive glass nanocomposite foam by gel casting method as cell scaffold for bone tissue. Eurasian J Anal Chem 2018;13:em17.
34. Gupta S, Jawanda MK, Sm M, et al. Qualitative histological evaluation of hard and soft tissue components of human permanent teeth using various decalcifying agents - a comparative study. J Clin Diagn Res 2014;8:ZC69-72.
35. Brunello G, Panda S, Schiavon L, et al. The Impact of Bioceramic Scaffolds on Bone Regeneration in Preclinical In Vivo Studies: A Systematic Review. Materials (Basel) 2020;13.
36. El-Rashidy AA, Roether JA, Harhaus L, et al. Regenerating bone with bioactive glass scaffolds: A review of in vivo studies in bone defect models. Acta Biomater 2017;62:1-28.
37. Denry I, Goudouri OM, Harless J, et al. Rapid vacuum sintering: A novel technique for fabricating fluorapatite ceramic scaffolds for bone tissue engineering. J Biomed Mater Res B Appl Biomater 2018;106:291-9.
38. Seyedmajidi M, Rabiee S, Haghanifar S, et al. Histopathological, histomorphometrical, and radiographical evaluation of injectable glass-ceramic-chitosan nanocomposite in bone reconstruction of rat. Int J Biomater 2015;2015:719574.
39. Mansoorianfar M, Mansourianfar M, Fathi MH, et al. Surface modification of orthopedic implants by optimized fluorine-substituted hydroxyapatite coating: Enhancing corrosion behavior and cell function. Ceramics International 2020;46:2139-46.
40. Saginova D, Tashmetov E, Tuleubaev B, et al. Effect of Platelet-rich Plasma Combined with Marburg Bone Bank-prepared Bone Graft in Rabbit Bone Defect Model. Shiraz E-Medical Journal 2023;24.
41. Macedo NL, Matuda Fda S, Macedo LG, et al. Bone defect regeneration with bioactive glass implantation in rats. J Appl Oral Sci 2004;12:137-43.
42. Gamal AS, Ali MA, Osama FA, et al. Histological study of the effect of bioactive glass on tibial bone repair in rats. Int J Clin Dev Anatomy 2015;1:13-21.
43. Reis CHB, Buchaim RL, Pomini KT, et al. Effects of a Biocomplex Formed by Two Scaffold Biomaterials, Hydroxyapatite/Tricalcium Phosphate Ceramic and Fibrin Biopolymer, with Photobiomodulation, on Bone Repair. Polymers (Basel) 2022;14.
44. Taktak R, Elghazel A, Bouaziz J, et al. Tricalcium phosphate-Fluorapatite as bone tissue engineering: Evaluation of bioactivity and biocompatibility. Mater Sci Eng C 2018;86:121-8.